Integrated Geophysical Approach to Aquifer Delineation in Crystalline Basement Environment

[1]AKINRINADE Opeyemi Joshua, [2]OLABODE Oladunjoye Peter

Abstract - Aquifer delineation and characterization could be somewhat challenging in Crystalline Basement Complex environment, where they are associated with either saturated weathered Basement or fractured Basement. Increasing demand for water occasioned by domestic and industrial purposes resulted in delineation and characterization of aquifer properties at a site within the crystalline basement environment, where two boreholes have been drilled (BH1 and BH2). Very Low Frequency Electromagnetic (VLF-EM) and Electrical resistivity methods were used. Twelve (12) VLF-EM profiles of length 120 – 160 m, with 10 m station separation oriented in east-west direction and twenty-five (25) VES stations were occupied. Three peak positive raw/filtered real VLF-EM anomalies identified are presumed to be water-filled fractures or faults; thus implying possible locations suitable for groundwater development. Four geoelectric layers were delineated namely: top soil, clayey sand/sandy clay, weathered layer and basement rock. The weathered layer is characterized by resistivity values which range from 28 to 1309 Ωm, and thickness values of 2.9 to 15.1 m. Longitudinal unit conductance (S), Transverse unit resistance (T), and coefficient of Anisotropy (λ) have values ranging from 0.03 – 0.16 mhos, 382 – 8517 Ωm2, and 1.05 – 2.24 respectively. These results are indicative of the aquifer protective capacity, hydraulic conductivity, aquifer productivity and hydrogeologic significance. BH1 failed because it was drilled into the weathered basement at a location characterized by fairly low transverse resistance, while BH2 was drilled into a localized fractured basement with fairly high recharge attributed to extent of fracture network, high transverse resistance and coefficient of anisotropy. Thus, fracture network and its depth extent are of great importance in selecting fractured basement aquifer as groundwater development site. Integration of electromagnetic profiling with electrical resistivity methods has shown to be complimentary tools in determination of groundwater potential and reduces uncertainties in predicting drillable positions. Robust assessment of the weathered basement and fractured basement aquifer parameters has assisted in locating productive borehole position in basement complex environment. This creates opportunities for efficient resources management, and reduces the risk of sinking unproductive boreholes.

Index Terms: Aquifer, Coefficient, Conductivity, Crystalline Basement Complex, Electrical Resistivity, Fracture, Groundwater, Very Low Frequency Electromagnetic.

1 INTRODUCTION

There is a continual increase in demand for portable water to meet both domestic and industrial uses. However, meeting this demand could be somewhat challenging in crystalline basement complex environment where aquifers are associated with either saturated weathered basement or linear structures such as fractures and faults within the basement rock (Odusanya and Amadi 1990;-Olayinka and Olorunfemi, 1992; Olorunfemi and Fasuyi, 1993;

Dan-Hassan and Olorunfemi, 1999; Adepelumi et al, 2013). The aquifers are not only inhomogeneous but also localized which makes characterization difficult (Ogungbemi and Oladapo, 2014). Furthermore, several factors influence the development of potential aquifer amongst which are: thickness of the saturated weathered layer and overburden thickness, aquifer depth and spacial extent, fracture network, and aquifer geometry. The volume of water stored in the aquifer, its vulnerability and rechargeability is dependent of the factors listed. Thus, detail characterization of the hydrogeophysical and hydrogeological properties is crucial in order to minimize risk of drilling unproductive boreholes.

In crystalline basement complex environment, integrated geophysical study using Very Low Frequency-Electromagnetic (VLF-EM) and Electrical Resistivity methods can assist in characterizing subsurface earth materials and modeling aquifer

- *[1]Akinrinade Opeyemi is currently an Assistant Lecturer at the Department of Marine Science and Technology, Federal University of Technology Akure, Nigeria, PH-+2347062522202. E-mail: ojakinrinade@futa.edu.ng*
- *[2]Olabode Oladunjoye is currently an Assistant Lecturer at the Department of Geophysics, Federal University Oye-Ekiti, Nigeria, PH-+2348032578542. E-mail: oladunjoye.olabode@fuoye.edu.ng*

units (Olayinka et al, 2004; Bayewu et al, 2012). This provides unique approach to determination of depth to saturated zones, thickness of the overburden, basement rock configuration, layer resistivity; vertical features such as fracture zones and geologic contacts (Greenhouse and Harris, 1983). Determination of these parameters provide viable tool for groundwater exploration (Bayewu et al, 2012).

Aquifers with low thickness values are characterized by low yield or none at all. This implies that aquifer thickness play a critical role in productivity within the basement complex terrain (Satpathy and Kanungo, 1976; Olorunfemi and Olorunniwo, 1985). However, high conductivity values does not necessarily imply a groundwater resource apart from deep weathering, such as high conductivity could result from a predominantly clayey regolith (Olayinka et al, 2004; Onu and Ibezim, 2004).

Transmissivity is an hydrogeologic parameter which is proportional to the permeability and thickness of aquifer. Transverse resistance (T) is a geophysical parameter which is proportional to resistivity and thickness of an aquifer. Hence, a linear relationship exists between transmissivity, permeability and transverse resistance (Harb et al 2010; Nafez et al., 2010). High quality aquifer is characterized by high transmissivity. Determination of the basic formation characteristics namely hydraulic conductivity and aquifer geometry is important for quantitative assessment of groundwater potential in crystalline basement environment. Areas with high transverse resistance are equivalent to areas with high hydraulic transmissivity and storage coefficient (Onu and Ibezim, 2004). Increase in longitudinal conductance (S) values may be attributed to increase in clay content and consequently a decrease in transmissivity. Therefore, longitudinal unit conductance can provide requisite and valuable information about aquifer protective capacity, because the earth as a system acts as natural filter to fluid flowing through it. Aquifers with sealing overburden have been characterized by high longitudinal unit conductance values (Jayeoba and Oladunjoye, 2013). Anisotropy represents change in measured property with direction. Thus, high anisotropic values are representative of high inhomogeneity, while low values represent fairly homogenous materials. Determination of transverse resistance, longitudinal conductance and anisotropy which have hydrogeological significance on aquifer productivity can be determined from the first order parameters namely resistivity and thickness. Thus, successful exploration and exploitation of groundwater requires a proper understanding of aquifer hydrogeologic characteristics (Ogungbemi and Oladapo, 2014).

Since most crystalline basement rocks are naturally poor aquifers as they lack essential hydraulic characteristics required for the storage and transmission of groundwater (Salami and Obrike, 2004), thorough geophysical investigation must be carried out in order to locate a viable drillable position for groundwater development. Aquifer porosity and permeability are created by secondary processes such as weathering, fractures, and joints etc. This results in anomalous distribution of aquifer properties, hydraulic conductivity and transmissivity of fluid in a typical basement complex aquifer system. The aim of this research is to delineate basement complex aquifer types, characterize the aquifer properties and its groundwater potential.

1.1 Description of the Study Site

The study site is situated in Akure, Southwestern Nigeria (Figure 1) and bounded by Longitude 5° 13′ 56.97″ E and 5° 14′ 02.05″ E; and Latitude 7° 15′ 33.63″ N and 7° 15′ 39.90″ N. Four factory buildings are constructed on the site, while granitic rock

outcrops are visible on the western flank. A hand dug well is located at the north-east, just outside the boundary wall, and an abandoned borehole is located at the north-western flank. There are vegetations within the site.

1.2 Geology of the Study Area

The study area is underlain by crystalline rocks of Precambrian Basement Complex of Southwestern Nigeria (Adegoke, 1972; Oyawoye, 1972; Rahaman, 1976). In the study location, Porphyritic granite is the major outcrop (Figure 2). Weathering processes have created a superficial layer that obscure the basement in the study site, except where the basement outcrop in the western flank.

2 METHODOLOGY

Ohmega resistivity meter, reels of cables, Hammers, Measuring tape, galvanized electrodes, Garmin Global Positioning System (GPS), and ABEM WADI VLF electromagnetic equipments were used for data acquisition, while Karous Hjelt filter, Win-Resist and surfer were used for data processing, modeling and visualization. Satellite imagery of the location was used for field preparation and survey planning. Twelve (12) profiles were cut in east-west orientation for the VLF-EM reconnaissance survey; with length range from 120 m to 160 m and ten (10) meters station spacing (Figure 3).

VLF-EM method makes use of the ground response to the propagation of electromagnetic fields which is composed of alternating electric intensity and magnetizing force. It does not require contact with the ground which thus facilitates its easy deployment and time saving advantage as compared with the electrical resistivity method. The main magnetic field component is horizontal and theoretically is to circle concentric about the antenna mast. Hence, it is irregular; it transmits in the range of 15-25KHz. This method compares the magnetic field of the primary signal (Transmitter) to that of the secondary signal (induced current flow within the sub surface electrical conductor). During the survey, raw real, filtered real, raw imaginary and filtered imaginary component of the EM signal was measured.

The measured filtered real (FR) and filtered imaginary (FI) were plotted against station position. Data filtering was carried out using Karous-Hjelt filter to enhance signal to noise ratio, such that tilt-angle crossovers will be easier to identify (Karous and Hjelt, 1983). The filter converts tilt-angle crossovers into peaks, and calculates the equivalent source current at a given depth, commonly known as current density. Current density was plotted with respect to depth with the aid of Karous-Hjelt program to create a pseudo-section for further interpretation. The current density assists in the interpretation of the width and dip of a fracture as a function of depth (Yusuf et al, 2015). Qualitative interpretation was carried out on the processed VLF data, using the raw and filtered real components plotted against station positions along the profiles. Field data obtained are presented as profiles and pseudo-sections.

Conventional electrical resistivity method using Vertical Electrical Sounding (VES) field procedure involves the introduction of current into the ground through galvanized electrodes, while the potential drop is measured with the aid of potential electrodes positioned between the current electrodes. The current and potential electrodes were expanded about a fixed centre, so as to probe deeper subsurface structures. The output resistances are averaged over a number of cycles; from each of these resistances the apparent resistivity for a particular spread length is computed using the relevant geometric factor (K). Using Schlumberger electrode array the current

electrode separation (AB/2) was varied from 1-100 m.

Twenty-five (25) VES stations, positioned at the peak positive raw/filtered real VLF-EM anomalies identified were occupied; aimed to delineating the geoelectric properties. VES 24 (BH1) was established at the location of the unproductive borehole and VES 23 at BH2 (Figure 3). The apparent resistivity values obtained were plotted against electrode spacing on a log-log graph. Partial curve matching using 2-layer master curves and the corresponding auxiliary curves (Keller and Frischknecht, 1966) to determine layer resistivity and thicknesses was carried. Obtained layers parameters were inverted with the aid of computer aided iteration using WinResist (Vander Velpen, 1988). Result of the quantitative interpretation and second order parameters estimated are presented in Table 1 and 2.

3 RESULT AND DISCUSSION

The results obtained from this study are presented as profiles, pseudo-sections, depth sounding curves, geoelectric sections, isoresistivity maps, isopach maps, second order parameters and tables.

VLF-EM profiles and pseudosections reveal the lateral and depth disposition of the current density along the profile lines occupied. The positive peaks are characterized by vertical structures as presented in the pseudosection plots (Figure 4a and b). The maximum depth probed was 20 m. Raw real component have values which range from -13.3 to 6.5, while the filtered real component range from -9.8 to 10.6. Regions of positive raw and filtered real component on the 2D maps (Figure 5a and b) were representative of linear structures which can serve as conduit for groundwater. Three anomalies were identified in the northeast (NE), northwest (NW) and southwestern (SW) flanks. The southwestern flank anomaly is considered to be a network of conductive linear structures extending northward, while that on the northeast and northwest are localized. The high positive raw/filtered real anomalies are presumed water-filled fractures or faults; implying possible locations suitable for groundwater development. The central part of the site is characterized by resistive structure, which is attributed to the basement rock.

Four resistivity sounding curve types were obtained; namely HA, KH, HK, and A (Figure 6, Table 1). Four geoelectric units typical of the geologic succession in a crystalline basement complex environment namely topsoil, clayey sand/sandy clay, weathered layer and basement rock were delineated. From the quantitative interpretation of the sounding curves, geoelectric sections, 2D iso-resistivity, layer thickness and overburden thickness maps were produced.

Geoelectric section one is 166 m long, with NW-SE orientation (Figure 7a). The thickness of the top soil varies across the profile, with highest at VES 8 and 14. Geoelectric section two is 148 m long, with SW-NE orientation (Figure 7b). The weathered layer resistivity varies between 49 and 1177 Ωm. The bedrock is closer to the surface between VES 8 and 10, resulting in the upward push of the weathered layer. The top soil is thicker on the SW flank of the profile. Geoelectric section three is 128m long, with SW-NE orientation (Figure 7c). The layer thickness distribution is appreciably less undulating. However, a depression is observed around VES 5, which affected the clayey sand/sandy clay and weathered layer. The top soil is fairly uniformly distributed, and the weathered layer relatively thin.

The top soil resistivity values range from 88 to 680 Ωm and thickness from 0.4 to 4.2 m (Figure 8a). The highest value was obtained around VES 5 in the south and VES 10 in the northeastern flank. The northwest is characterized by relatively low resistivity values. Resistivity values of the clayey sand/sandy clay (second geoelectric unit) range from

46 to 597 Ωm and thickness from 1 to 15.1 m (Figure 8b). The highest value was obtained around VES 6, having a northeast-southwest orientation. The northeastern and western flanks of the field are characterized by relatively low resistivity values. By implication, the site is characterized by relatively low grade competent earth materials.

The weathered layer (third geoelectric unit) resistivity values range from 28 to 1309 Ωm, with thickness from 2.9 to 15.1 m (Figure 9a). The highest resistivity values were obtained around VES 8 and 9 at the central part of the site and the northeastern flank. The southwestern and southeastern flank exhibit low resistivity values of less than 400 Ωm. Areas characterized by high thickness values within the third geoelectric unit, were observed to have relatively high resistivity values (Figure 9b). This confirms differential weathering at this site. For groundwater development purpose, the saturated weathered layer should be of appreciable thickness and relatively low resistivity values occasioned by the fluid content.

The bedrock resistivity value range from 626 to 16451 Ωm (Figure 10a). The central part of the site is characterized by high resistivity values. However, three low resistivity zones were observed within the basement rock. These are the northeastern flank; northwestern flank; and the southern flank which extend eastward. These low resistivity anomalies have similar pattern characterized by high conductivity values in raw/filtered real VLF-EM map (Figure 5a and b). Thus, these structures are presumed to be fractured bedrock. The overburden thickness range from 4.8 to 23.2 m. The central part of the site is characterized by low overburden thickness values of less than 10 m (Figure 10b). The general outlay shows that the site is characterized by relatively low overburden, which is not of appreciable thickness for groundwater development. However, high values were obtained at the western flank around VES 7 and on the southeast through northeastern flank.

Dar Zarrouk parameters were estimated using the layer resistivity and thickness values of each geoelectric units (Table 2). Longitudinal unit conductance values obtained range from 0.03 to 0.16 mhos (Figure 11a). Generally, the site is characterized by low longitudinal conductance values and thus exhibit low protective capacity implying aquifer vulnerability according to Henrieth (1976) and Oladapo (2004) classification. A low longitudinal conductance pattern which extends from the south through the centre to VES 9 is observed. This reveals area with possible highest vulnerability. This is corroborated by the open fracture observed in the VLF-EM Profile 1, between 80 and 100 m (Figure 4a) Transverse resistance values range from 382.22 to 8516.66 (Ωm^2) (Figure 11b), and has a direct relationship with transmissivity and permeability. Therefore, areas with high transverse resistance are associated with high transmissivity. The northeastern flank and the central section are characterized by relatively high transmissivity and permeability, which in turn influence aquifer recharge.

Estimated anisotropy coefficient range from 1.05 to 2.24 (Figure 12). The northeastern flank and central part around VES 9 is characterized by peak values. This indicates inhomogeneity of the geologic sequence and surrounding materials, or a product of pore fluid. Similar hypothesis applies to the fractured basement aquifer located around VES 9 (Figure10a). However, the fractured basement aquifer located at the southern flank is associated with low anisotropy coefficient values, representing fairly homogenous earth materials.

4 CONCLUSION

This study demonstrates the use of VLF-EM and electrical resistivity methods to delineate aquifer types in basement complex environment. Obtained results provide qualitative information on the hydrogeologic framework and subsurface disposition of aquifer units. Reconnaissance survey using VLF-EM provide a non-intrusive approach to delineate linear features such as fractures and faults in the fractured basement. These linear features are potential conduit and reservoir for groundwater in basement complex environment. Four geoelectric layers consisting of top soil, clayey sand/sandy clay, weathered layer and basement rock were delineated. Generally, the thickness of the weathered layer is low, which makes it not reliable target for groundwater development. Areas within the basement rock characterized by high raw/filtered real values have similar pattern with that of the low resistivity anomaly delineated in the fractured basement, which thus reveal that VLF-EM anomalies are not representative of the overburden thickness.
BH1 (VES 24) failed because it was drilled to abstract groundwater from the weathered layer, at a location characterized by low raw/filtered real values, on the flank of a localized network of fractures within the bedrock. Base on the transverse unit resistance and coefficient of anisotropy values, recharge and groundwater flow direction is towards VES 9. BH2 (VES 23) was drilled into the fractured basement with fairly high recharge attributed to the high transverse resistance and extent of the fracture network. Therefore, fracture network and its depth extent are of great importance in selecting fractured basement aquifer as groundwater development site.

Integration of electromagnetic profiling with electrical resistivity methods serve as complimentary tool in determination of groundwater potential and reduces uncertainties in predicting drillable positions. For productive borehole in basement complex environment, robust assessment of the weathered basement and fractured basement aquifer parameters should be carried out. This will create opportunity for efficient resources management, and reduce the risk of sinking unproductive boreholes.

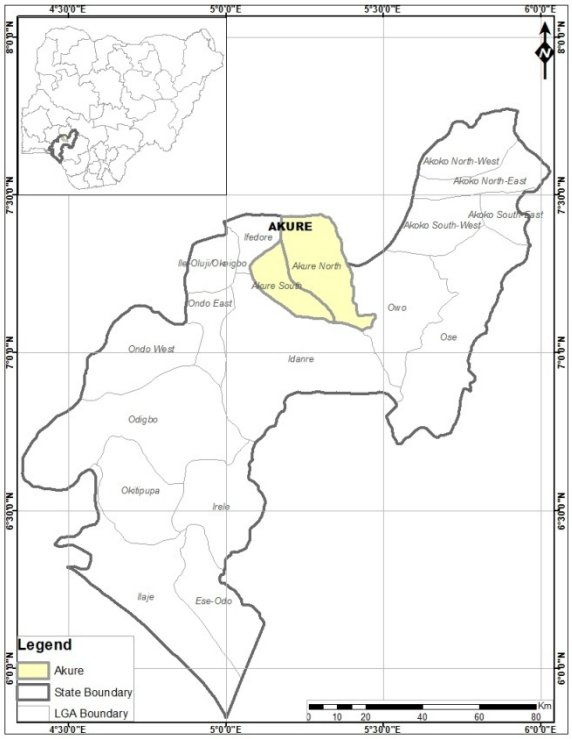

Figure 1: The Map of Ondo state showing the study site (modified after Mogaji et al, 2011).

Figure 2: Simplified Geological map of Akure (Modified after Owoyemi, 1996)

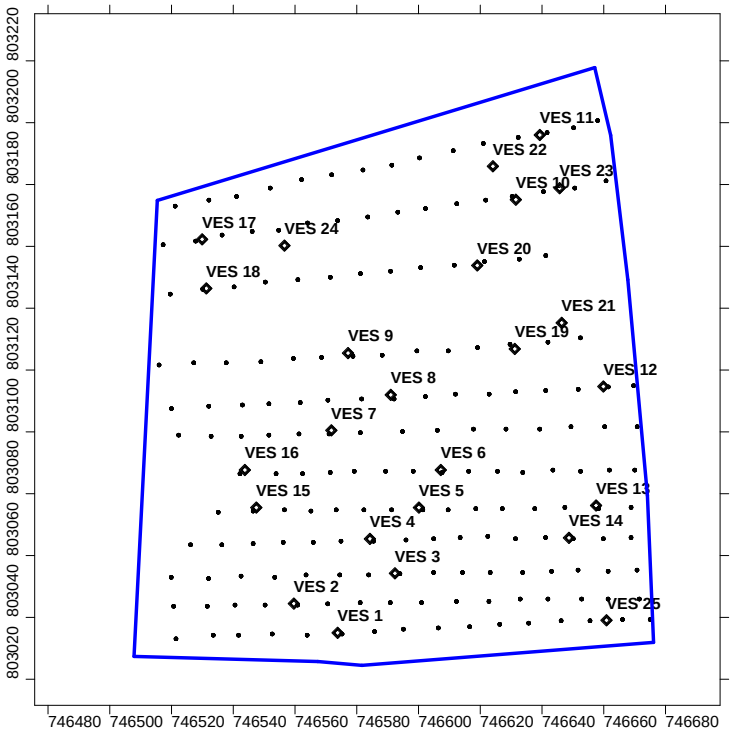

Figure 3: Base map of the study area showing the survey layout.

Table 1: Summary of geo-electric parameters over the study area

VES Station	No. of layers	Resistivity (Ohm-m) $\rho_1/\rho_2/\ldots\rho_{n-1}$	Curve Type	Thickness(m) $h_1/ h_2/ h_3$	Depth(m) $d_1/d_2/\ldots d_{n-1}$
1	4	296.3/170.4/347.8/1300.8	HA	0.4/4.4/5.7	0.4/4.8/10.5
2	4	181.8/303.2/82.6/7157.5	KH	0.9/3.4/5.2	0.9/4.3/9.5
3	4	112/368.4/159.7/3599.6	KH	0.5/2.5/6.5	0.5/3.0/9.5
4	4	211.9/415.5/74.9/12345.6	KH	0.6/2.2/4.9	0.6/2.8/7.7
5	4	680.3/154.5/755.7/7140.9	HA	1.5/4.0/4.2	1.5/5.5/9.7
6	4	247.3/597.3/124/1654.1	KH	0.7/1.7/5.3	0.7/2.4/7.7
7	4	231.4/229.9/590.7/7427.0	HA	2.5/15.1/5.6	2.5/17.6/23.2
8	4	117.4/156/1158.8/16134.7	A	3.8/3.1/4.1	3.8/6.9/11
9	4	90.5/136/1309.1/1553.8	A	2/1.1/3.3	2/3.1/6.4
10	4	439.1/179.7/702.1/1004.2	HA	0.8/6.2/5.1	0.8/7.0/12.1
11	4	193.5/49.5/211.3/13042.2	HA	1.1/1.0/15.1	1.1/2.1/17.2
12	4	133.2/65.1/139.6/13672.5	HA	1.0/4.7/11.4	1.0/5.7/17.1
13	4	223.6/111.1/216.5/1632.5	HA	1.0/4.6/7.2	1.0/5.6/12.8
14	4	130.1/91.6/366.9/10084.3	HA	4.2/5.6/5.4	4.2/9.8/15.2
15	4	155.9/68.1/402.2/7905.4	HA	3.3/3.9/3.9	3.3/7.2/11.1
16	4	169.0/89.9/328.8/9249.3	HA	3.2/4.2/2.9	3.2/7.4/10.3
17	4	88.4/277.8/27.9/15281.7	KH	0.8/1.0/3.0	0.8/1.8/4.8
18	4	182.7/53.2/347.4/9965.5	HA	2.8/3.9/3.0	2.8/6.7/9.7
20	4	116.3/210.9/48.5/16450.6	KH	1.2/2.4/3.9	1.2/3.6/7.5
21	4	263.4/45.9/717.6/6859.6	HA	1.8/4.0/3.4	1.8/5.8/9.2
22	4	230.3/49.3/525.3/5243.1	HA	1.4/3.7/5.8	1.4/5.1/10.9
23	4	188.6/47.5/1177.4/625.5	HK	1.9/3.2/6.8	1.9/5.1/11.9
24	4	114.4/70.4/370.6/2921.0	HA	1.3/3.7/8.2	1.3/5.0/13.2
25	4	99.0/66.0/390.5/3364.6	HA	1.5/5.5/6.9	1.5/7.0/13.9

Table 2: Second order parameters determined from layer resistivity values and thicknesses.

VES No.	Longitudinal Conductance S (mS/m)	Transverse Resistance T (Ωm^2)	Anisotropy (λ)
VES 1	0.0436	2850.74	1.0613
VES 2	0.0791	1624.02	1.1932
VES 3	0.0520	2015.05	1.0770
VES 4	0.0735	1408.25	1.3217
VES 5	0.0337	4812.39	1.3120
VES 6	0.0484	1845.72	1.2277
VES 7	0.0860	7357.91	1.0841
VES 8	0.0558	5680.8	1.6182
VES 9	0.0327	4650.63	1.9271
VES 10	0.0436	5046.13	1.2257
VES 11	0.0973	3452.98	1.0659
VES 12	0.1614	2030.61	1.0586
VES 13	0.0791	2293.46	1.0525
VES 14	0.1081	3040.64	1.1930
VES 15	0.0881	2348.64	1.2961
VES 16	0.0745	1871.9	1.1463
VES 17	0.1210	382.22	1.4166
VES 18	0.0973	1761.24	1.3494
VES 20	0.1021	834.87	1.2311
VES 21	0.0987	3097.56	1.9007
VES 22	0.0922	3551.57	1.6599
VES 23	0.0832	8516.66	2.2372
VES 24	0.0860	3448.12	1.3049
VES 25	0.1162	3205.95	1.3883

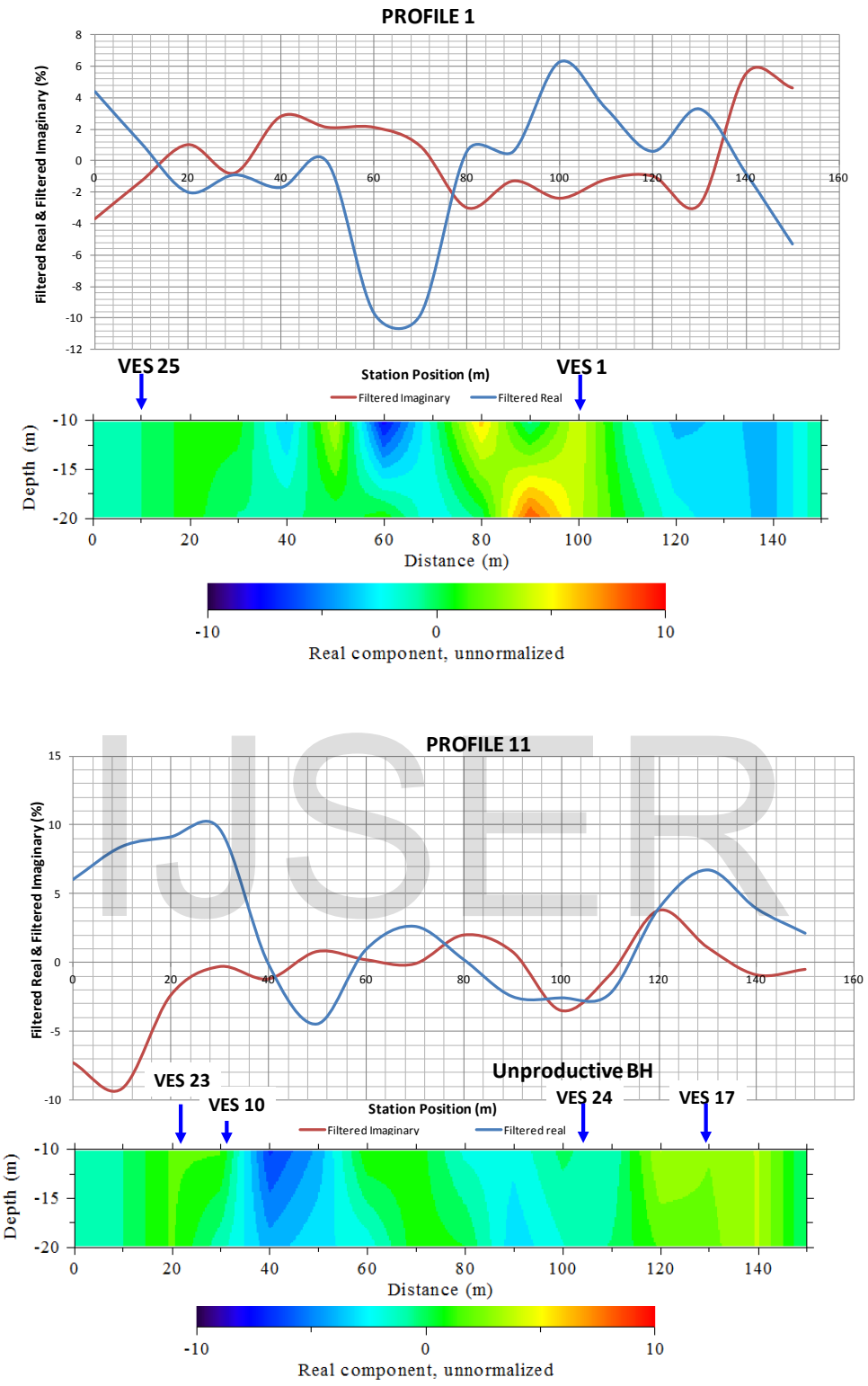

Figure 4: (a) VLF-EM profile 1 and the pseudo section with VES 25 and 1 indicated on the profile. (b) VLF-EM profile 11 and the location of the unproductive Borehole.

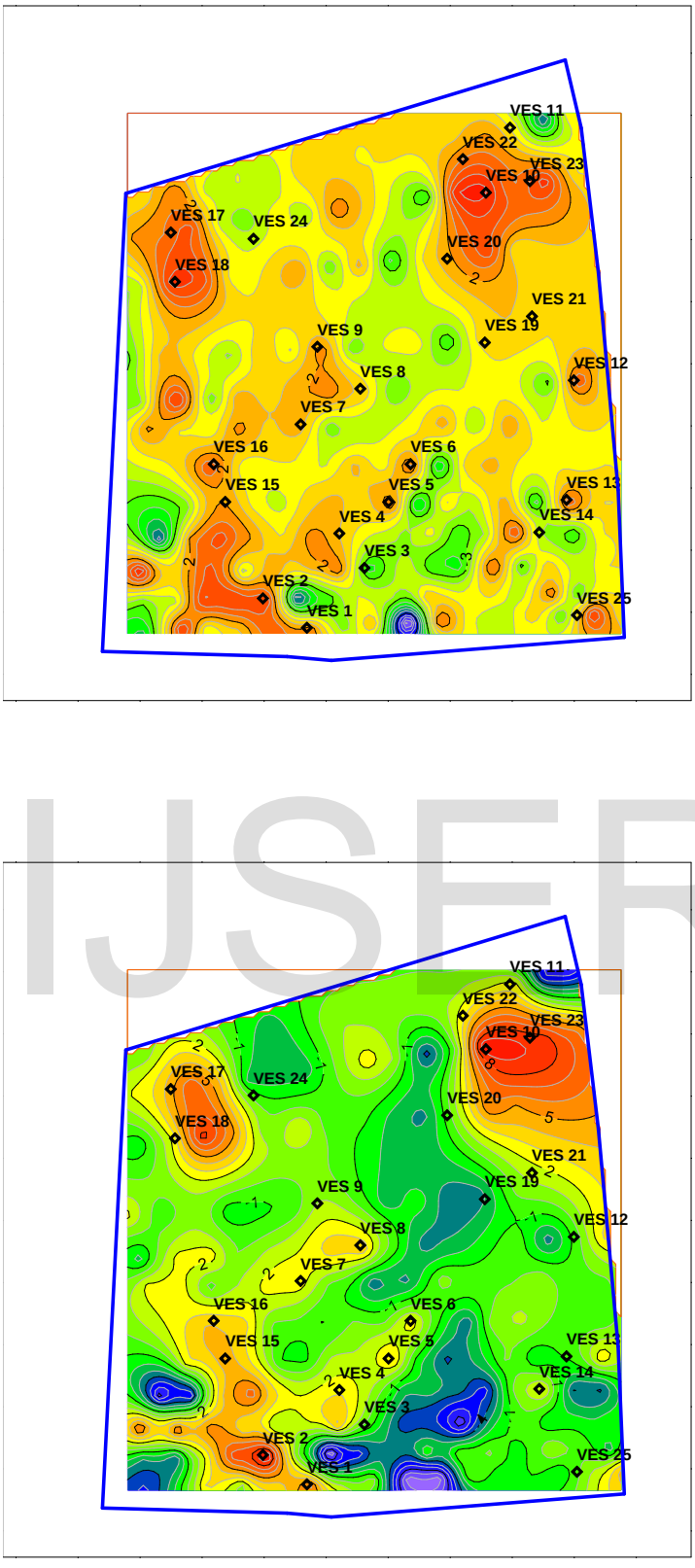

Figure 5: (a) 2D conductivity map of the raw real VLF-EM data acquired over the site (b) 2D conductivity map of the filtered real VLF-EM data acquired over the site

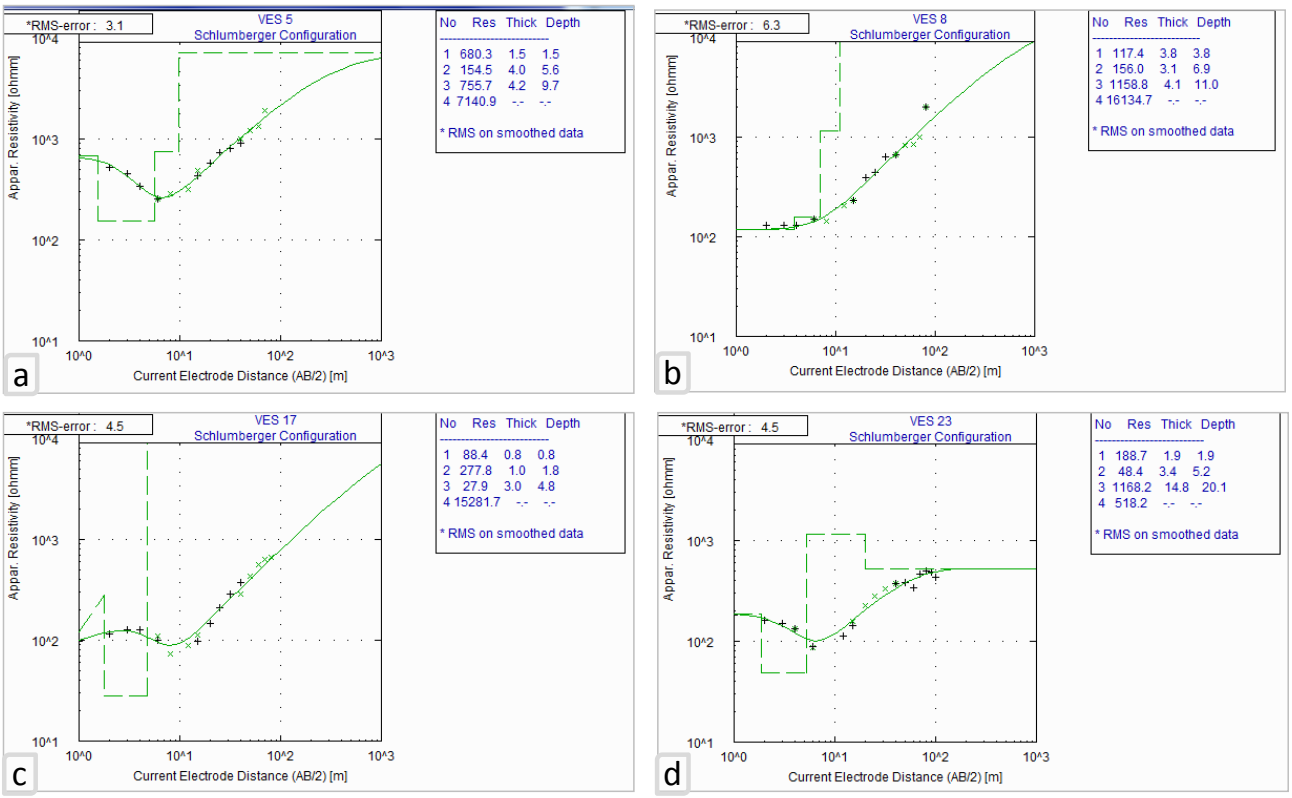

Figure 6: Representative Geoelectric Sounding Curves are (a) VES 5 Typical 'HA' curve (b) VES 8 Typical 'A' curve (c) VES 17 Typical 'KH' curve and (d) VES 23 Typical 'HK' curve

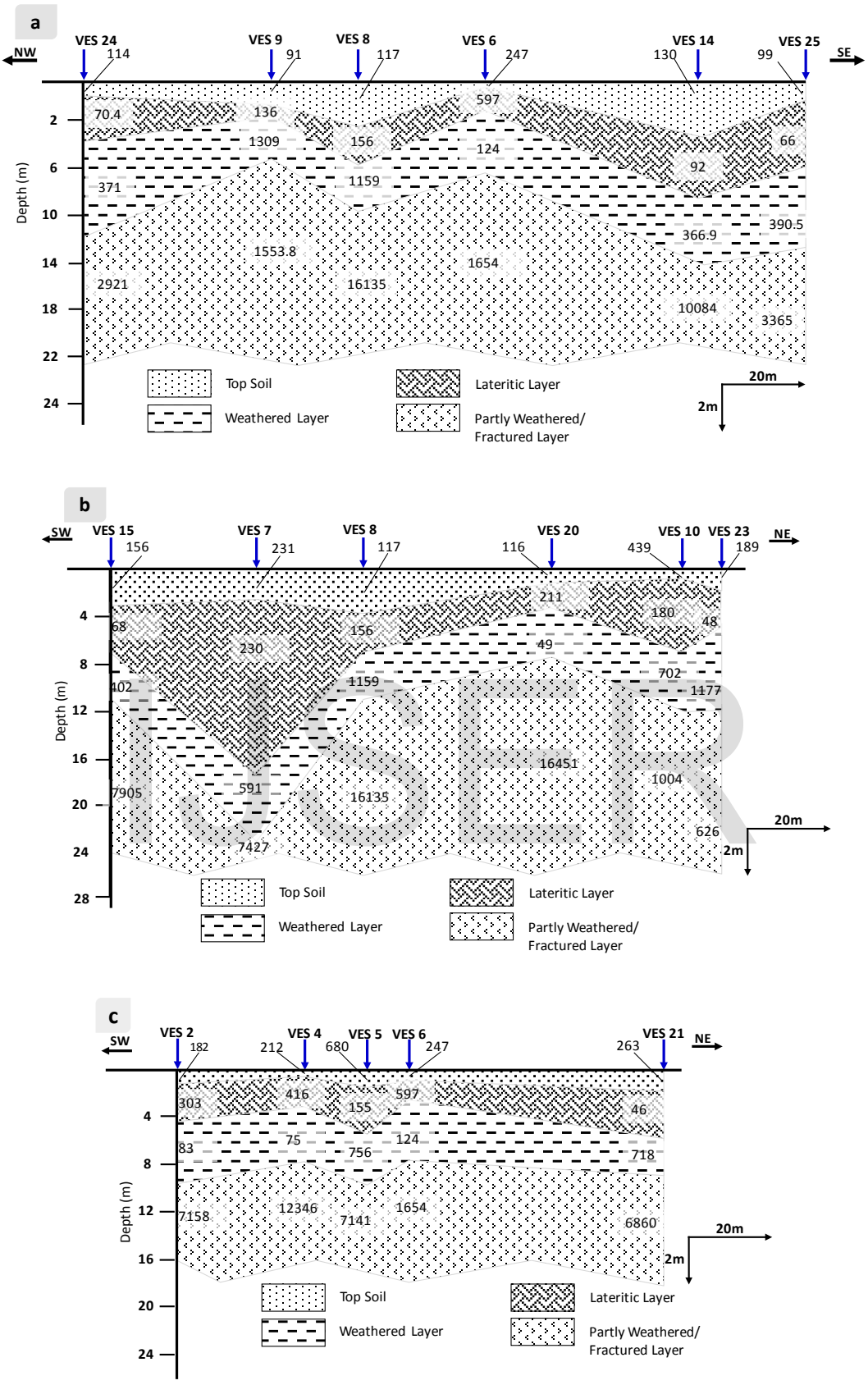

Figure 7: Geo-electric section along arbitrary lines (a) VES 24, 9, 8, 6, 14, and 25 (B) VES 15, 9, 8, 20, 10, and 23 and (c) VES 2, 4, 5, 6, and 21

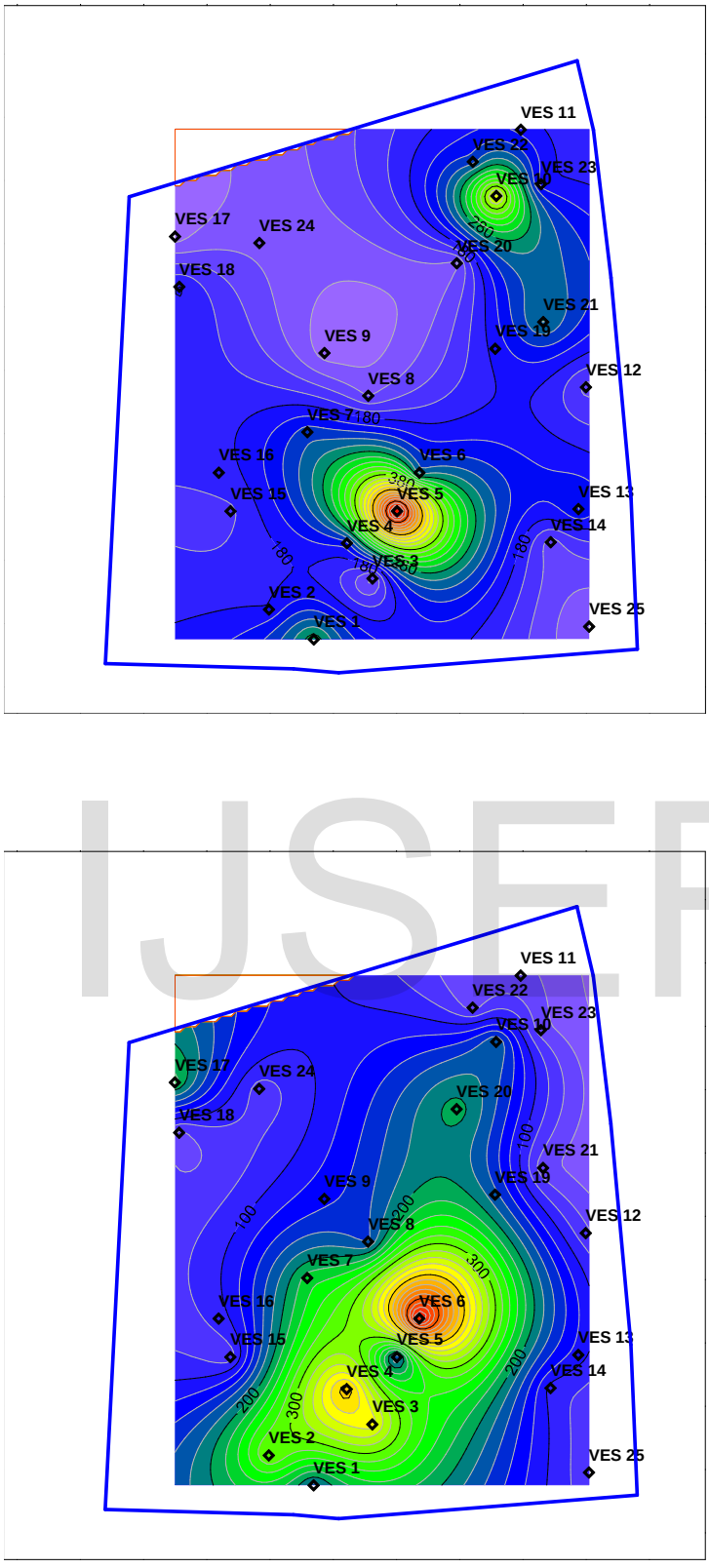

Figure 8: (a) Isoresistivity map of the first geoelectric layer (top soil) (b) Isoresistivity map of second geoelectric layer (Clayey sand/sandy clay)

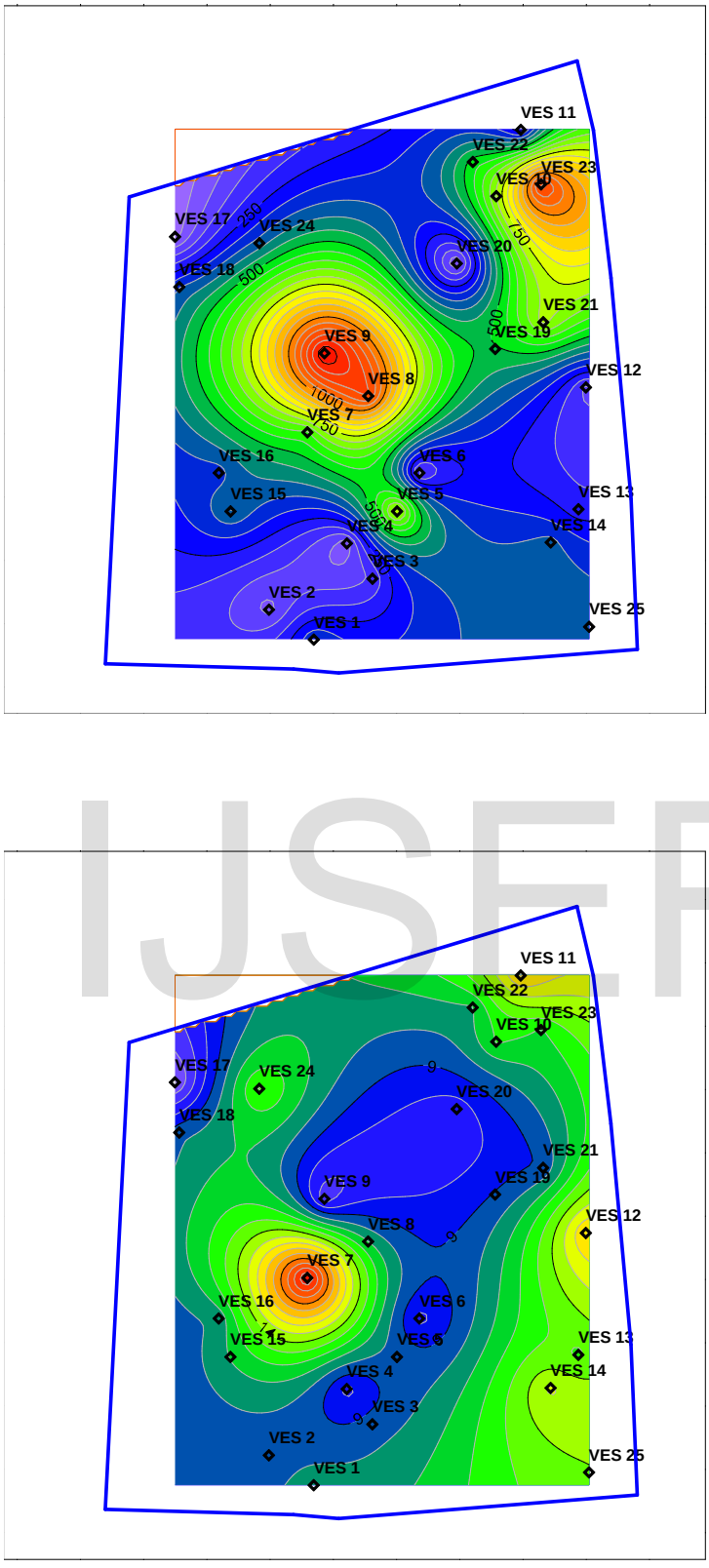

Figure 9: (a) Isoresistivity map of the third geoelectric layer (Weathered layer) (b) Isopach map of the overburden in the study area

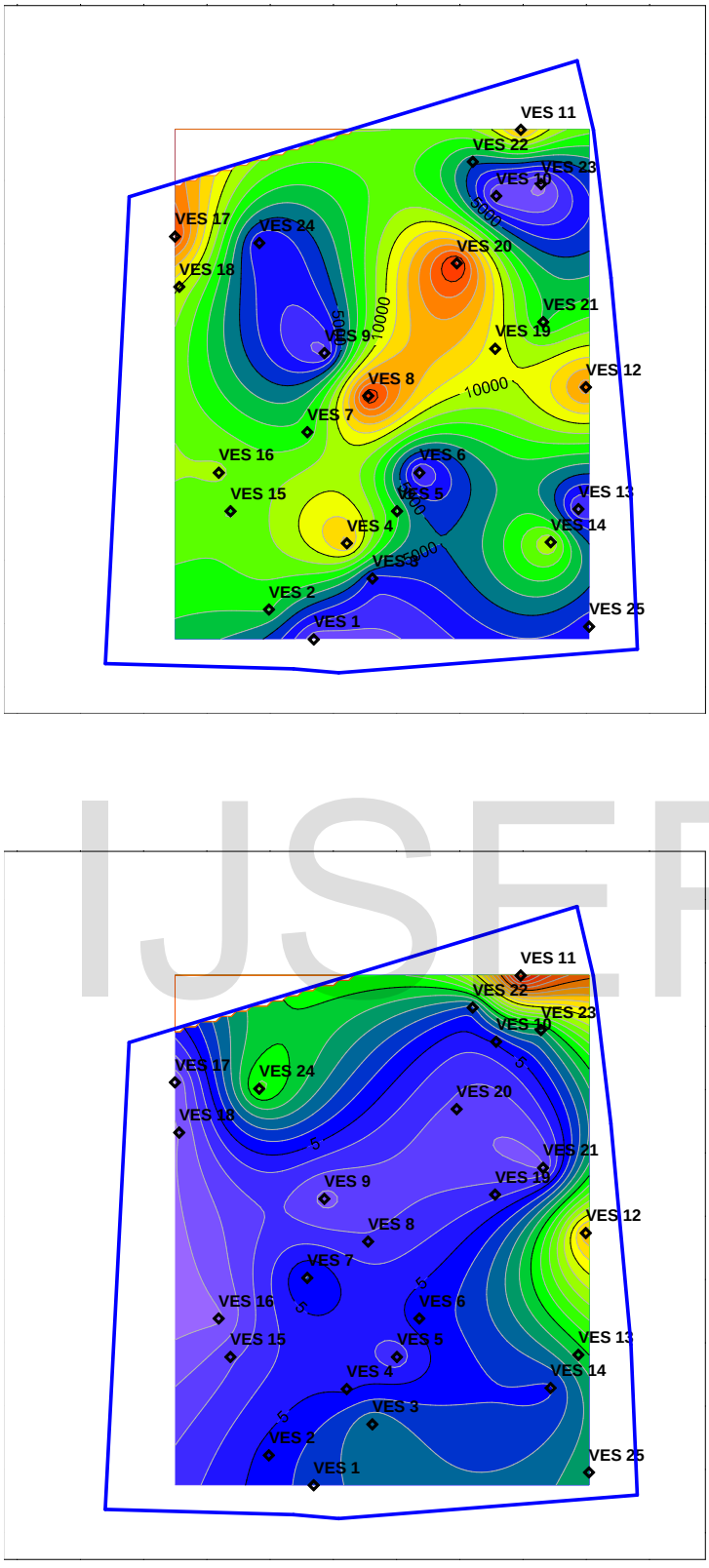

Figure 10: (a) Isoresistivity map of the fourth geoelectric layer (bedrock) (b) Isoapch map of weathered layer in the study site

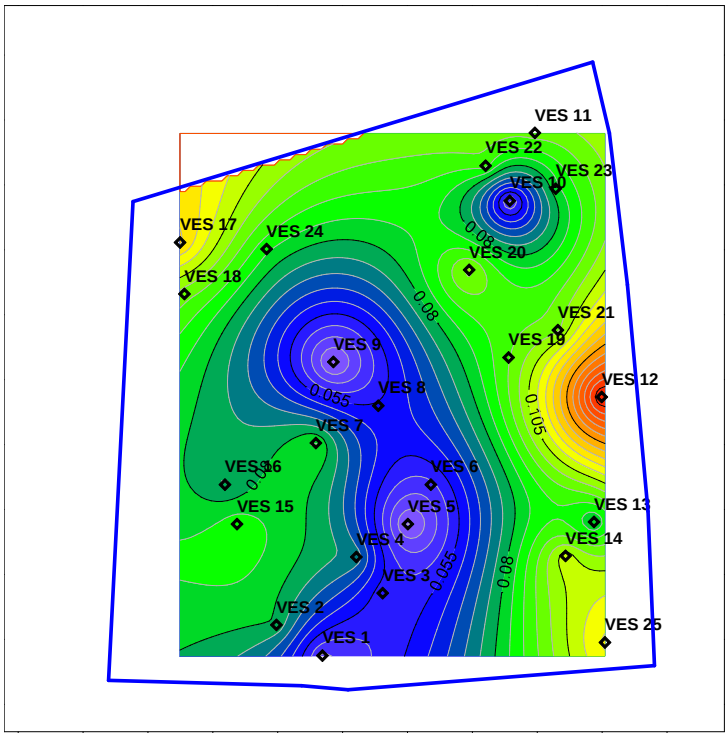

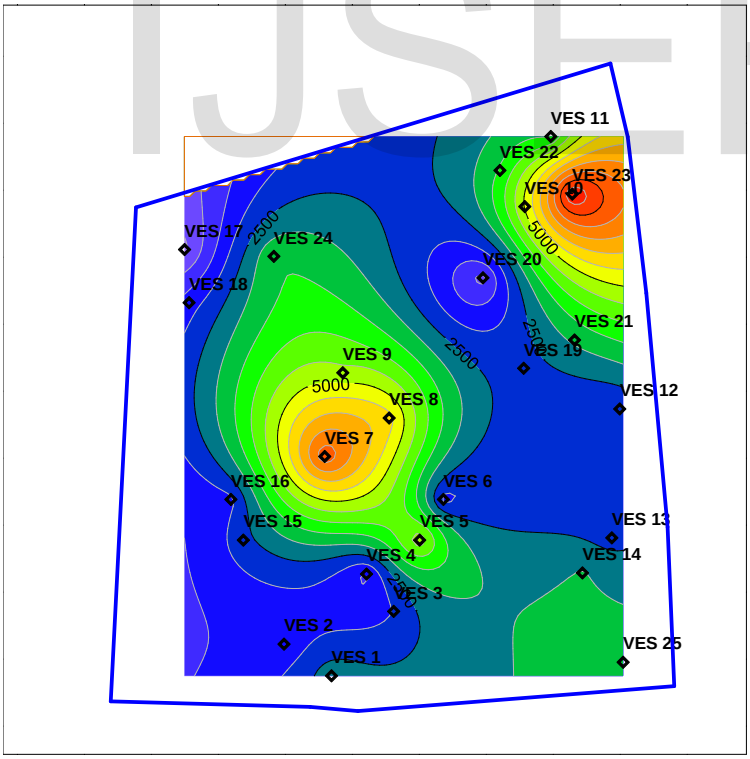

Figure 11: (a) Longitudinal unit conductance map of the study site (b) Transverse resistance map of the study site

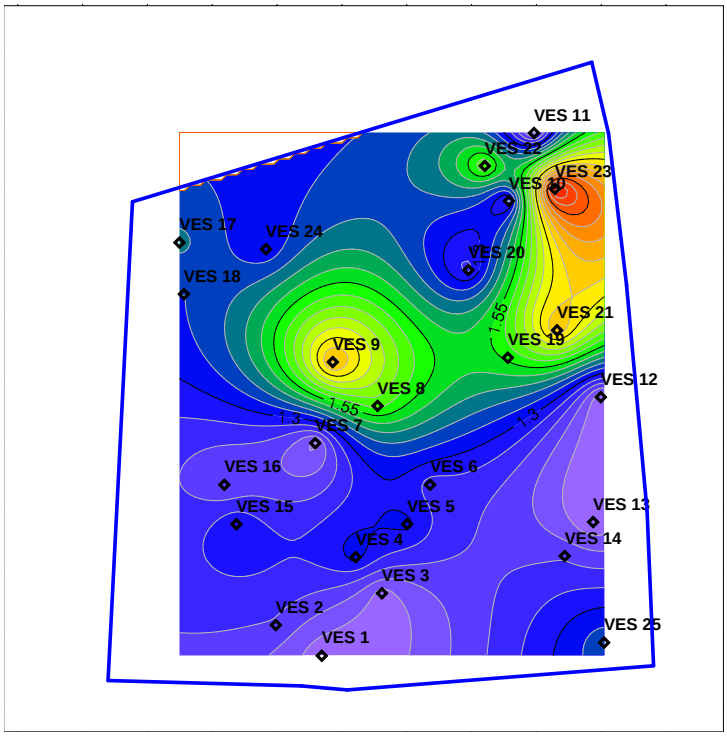

Figure 12: Anisotropy coefficient map of the study site

5 Acknowledgments

The authors wish to thank Mr. Kunle Akinlalu for his helpful comment and suggestion, also Mr. Olumide Akande for his assistance with site map preparation.

6 REFERENCES

[1] Odusanya B.O., Amadi U.N.P. "An empirical resistivity model for predicting shallow groundwater in the Basement Complex Water Resources," Journal of Nigeria Association of Hydrogeologists, Vol. 2, 77- 87, 1990.

[2] Olayinka, A. I. and Olorunfemi, M. O. Determination of geoelectrical characteristics in Okene area and implication for borehole siting. Journal of Mining and Geology, 28: 403-412, 1992.

[3] Olorunfemi, M. O. and Fasuyi, S. A. Aquifer types and the geoelectric /hydrogeological characteristics of part of the central basement terrain of Nigeria (Niger State). Journal of African Earth Sciences, 16 (3): 309-316, 1993.

[4] Dan-Hassan M.A., and Olorunfemi M.O. "Hydro-geophysical investigation of a basement terrain in the north central part of Kaduna State, Nigeria," Journal of Mining Geology, Vol. 35(2), 189-206, 1999.

[5] Adepelumi, A. A., Akinmade, O. B., Fayemi. O. Evaluation of Groundwater Potential of Baikin Ondo State Nigeria Using Resistivity and Magnetic Techniques: A Case Study, Universal Journal of Geoscience 1(2): 37-45, 2013.

[6] Ogungbemi, O. S., and Oladapo, M. I. Combined Use of Electromagnetic and Magnetic Survey for Hydrogeophysical Characterization of Ijapo Housing Estate, Akure, British Journal of Applied Science & Technology 4(7): 1138-1148, 2014.

[7] Olayinka, A.I, Amidu, S.A., and Oladunjoye, M.A. "Use of Electromagnetic Profiling and Resistivity Sounding for Groundwater Exploration in the Crystalline Basement Area of Igbeti, Southwestern Nigeria". *Global Journal of Geological Sci*. 2(2): 243-253, 2004.

[8] Bayewu O.O., Oloruntola M.O., Mosuro G.O., Watabuni F.G. Groundwater exploration in Ago-Iwoye Area of Southwestern Nigeria, using Very Low Frequency Electromagnetic (VLF-EM) and Electrical Resistivity methods. Int. Journal of Applied Sciences and Engineering Research, Vol. 1(3), 2012.

[9] Greenhouse, J.P. and Harris, R.D. DC, VLF and Inductive Resistivity surveys, in Cherry, J.A. (ad.), Migration of Contaminants in Groundwater at a Landfill: A Case Study, Journal of Hydrology, 63, pp. 177-197, 1983.

[10] Satpathy B.N., Kanungo B.N., "Groundwater Exploration in Hard rock terrain, a case study," Geophysical Prospecting, **Vol. 24**(4), 725-736, 1976.

[11] Olorunfemi M.O., Olorunniwo M.A., "Parameters and aquifer characteristics of some parts of SW. Nigeria," Geologic Applica E. Hydrogeological, XX Part 1, 99-109, 1985.

[12] Onu N. N. and Ibezim, C. U. Hydrogeophysical investigation of Southern Anambra Basin Nigeria. Global Journal of Geological Sciences, Vol. 2(2), 221-233, 2004.

[13] Harb, N., Haddad, K., and Farkh, S. Calculation Of Transverse Resistance To Correct Aquifer Resistivity Of Groundwater Saturated Zones: Implications For Estimating Its Hydrogeological Properties, Lebanese Science Journal, Vol. 11 (1), 105-115, 2010.

[14] Nafez, H., Kaita, H. and Samer, F. Calculation of transverse resistance to correct aquifers resistivity of groundwater saturated zones: Implication for estimated its hydrogeological properties. Lebanese Science Journal, 11(1), pp. 105–115, 2010.

[15] Jayeoba, A., Oladunjoye M. A. Hydro-geophysical evaluation of groundwater potential in hard rock terrain of southwestern Nigeria, RMZ – M&G, Vol. 60, pp. 271–285, 2013.

[16] Salami B. M., and Obrike. S.E. Effective borehole design in difficult crystalline rock terrain, a case study of the Abakaliki pyroclastic rocks, Global Journal of Geological Sciences, Vol. 2(2), 183-190, 2004.

[17] Adegoke O.S. "Thethyan affinities of West African Paleogene Molluscs," Proceedings, 24th International Geological Congress, Montreal, 1972.

[18] Oyawoye M.O. "The basement complex of Nigeria, In: Dessauvagie TFJ, Whiteman AJ (eds) African geology," Ibadan University Press, 1972.

[19] Rahaman M.A. "A Review of the Basement Geology of Southwestern Nigeria In Kogbe, C.A. (Editor)," Geology of Nigeria, Elizabethan Publishing Co., 1976.

[20] Karous M., Hjelt S.E. "Linear Filter of VLF Dip-Angle Measurements," Geophysical Prospecting, Vol. 31, 782-794, 1983.

[21] Yusuf G. A., Akinrinade O. J., Ojo J. S. An Engineering Site Characterization Using Geophysical Methods – A Case Study From Akure, Southwestern Nigeria, Journal of Earth Sciences and Geotechnical Engineering, (submitted for publication).

[22] Keller, G.V. and Frishnecht, F.D. *Electrical methods in Geophysical Prospecting*. Pergamon Press, New York, 1966.

[23] Vander Velper B.P.A. RESIST, version 1.0, a package for the processing of the resistivity data. ITC, Delf Netherland, 1988.

[24] Mogaji, K. A., Olayanju, G. M. and Oladapo, M. I. "Geophysical evaluation of rock type impact on aquifer characterization in the basement complex areas of Ondo State, Southwestern Nigeria: Geo-electric assessment and Geographic Information Systems (GIS) approach," International Journal of Water Resources and Environmental Engineering, **Vol. 3(**4), 77-86, 2011.